Virology 534 (2019) 25–35

Contents lists available at ScienceDirect

Virology

journal homepage: www.elsevier.com/locate/virology

Three ourmia-like viruses and their associated RNAs in *Pyricularia oryzae*

Shuhei Ohkita[a,1], Yui Lee[a,1], Quyet Nguyen[a], Kenichi Ikeda[a], Nobuhiro Suzuki[b], Hitoshi Nakayashiki[a,*]

[a] Laboratory of Cell Function and Structure, Graduate School of Agricultural Science, Kobe University, Nada Kobe, 657-8501, Japan
[b] Agrivirology Laboratory, Institute of Plant Science and Resources, Okayama University, Kurashiki, Okayama, 710-0046, Japan

ARTICLE INFO

Keywords:
Ourmia-like virus
Subviral RNA
Mycovirus

ABSTRACT

Three ourmia-like viruses, designated Pyricularia oryzae ourmia-like virus (PoOLV) 1 to 3, were identified in a wheat-infecting isolate of *P. oryzae*. The sizes of the full-length PoOLV1-3 genomes were determined to be 2,528, 1,671, and 2,557 nt. Interestingly, we also found two abundant single-stranded RNAs sharing their 5' terminal 25 and 255 nt with PoOLV1 RNA and PoOLV3 RNA, respectively. The PoOLV1- and PoOLV3-associated RNAs (ARNA1 and ARNA3) were 639 and 514 nt in length, and possessed one and two small ORFs, respectively. In the field isolates of *P. oryzae*, PoOLVs and ARNAs were detectable at varying levels, and the levels of PoOLV1 and ARNA1 as well as those of PoOLV3 and ARNA3, were tightly correlated. In addition, gene silencing of PoOLV1 and PoOLV3 resulted in a reduction of ARNA1 and ARNA3, respectively. There results indicated that replication of ARNA1 and ARNA3 was associated with PoOLV1 and PoOLV3, respectively.

1. Introduction

Ourmiavirus is a genus of plant viruses infecting melon, cherry, and cassava (Lisa et al., 1988; Turina et al., 2017). The members of *Ourmiavirus* have unique bacilliform virions containing three linear single-stranded positive-sense RNAs (RNA1-3). Three viral proteins, RNA-dependent RNA polymerase (RdRP), movement protein (MP), and capsid protein (CP) are encoded by RNA1, 2 and 3, respectively.

Interestingly, phylogenetic analysis revealed that RdRPs of ourmiaviruses are distantly related to RdRPs of common plant viruses but showed the closest similarity with yeast viruses of the genus *Narnavirus* (Rastgou et al., 2009). In contrast, MPs and CPs of ourmiaviruses clustered with those of plant viruses (Rastgou et al., 2009). In particular, their MPs showed clear similarities with the MPs of viruses in the *Tombusviridae* family. Based on these studies, it was proposed that *Ourmiavirus* might have evolved by inter-kingdom reassortment of viral genome segments (Rastgou et al., 2009).

Narnavirus is a genus in the family *Narnaviridae*. Members of *Narnaviridae* are among the simplest of RNA viruses having only a 2.3–3.6 Kb positive single stranded RNA that encodes a single protein, RdRP for their own replication (Hillman and Cai, 2013). Therefore, the members of *Narnaviridae* do not have a capsid. Genetic and biochemical evidence indicated that narnaviruses replicate in the cytoplasm (Solorzano et al., 2000). In contrast, members of *Mitovirus*, the other genus in *Narnaviridae*, are thought to replicate in mitochondria since they often use mitochondrial genetic code (Hong et al., 1998; Polashock and Hillman, 1994).

While members of the family *Narnaviridae* are regarded as a group of mycoviruses, with the development of high throughput sequencing technology, narna-like sequences have been detected in a wide range of eukaryotes including filamentous fungi, oomycetes, invertebrates, and plants (Bruenn et al., 2015; Cai et al., 2012; Donaire et al., 2016; Illana et al., 2017; Mu et al., 2018; Shi et al., 2016). One of such elements is fungal ourmia-like viruses. While RdRP-based phylogenetic analysis indicated that the ourmia-like viruses are more closely related to the plant *Ourmiavirus* rather than to the yeast *Narnavirus* (Donaire et al., 2016; Illana et al., 2017; Shi et al., 2016), they are believed to have a single genomic RNA encoding RdRP as do narnaviruses. Therefore, the simple genome organization of the ourmia-like viruses favors the idea that they belong to *Narnaviridae* rather than to *Ourmiavirus*.

The ascomycetous fungus *Pyricularia oryzae* (Syn., *Magnaporthe oryzae*) is the causal agents of blast disease on various gramineous plants including rice, wheat, oat, and finger millet, among others (Ikeda et al., 2019). Generally, each isolate has a very limited host range, and isolates from different host plants are genetically distinguishable.

A wide variety of mycoviruses have been identified in

* Corresponding author. Laboratory of cell function and structure, Graduate School of Agricultural Science, Kobe University, Rokkodai-cho, Nada, 657-8501, Kobe, Japan.
E-mail address: hnakaya@kobe-u.ac.jp (H. Nakayashiki).
[1] These authors contributed equally to this work.

https://doi.org/10.1016/j.virol.2019.05.015
Received 20 July 2018; Received in revised form 20 May 2019; Accepted 24 May 2019
Available online 25 May 2019
0042-6822/

phytopathogenic fungi (Ghabrial and Suzuki, 2009). Among them, mycoviruses belonging to Totiviridae and Chrysoviridae have been found in *P. oryzae* (Maejima et al., 2008; Urayama et al., 2010). In addition, unassigned mycoviruses related to *Ourmiavirus* and plant viruses of the family *Tombusviridae* were also identified (Ai et al., 2016; Illana et al., 2017; Li et al., 2019). Notably, Magnaporthe oryzae chrysovirus 1 (MoCV1)-A and -B were shown to reduce the ability of the host fungus to cause disease in plants as well as to grow on rich media, making MoCV1-A and –B potential biocontrol agents (Urayama et al., 2010, 2012, 2014). These *P. oryzae* mycoviruses were all isolated from rice-infecting isolates. Thus, the full virome in *P. oryzae,* especially that in non-rice infecting isolates, remains to be explored.

In this study, using Illumina sequencing, three ourmia-like viruses, Pyricularia oryzae ourmia-like virus 1 to 3 (PoOLV1-3) were found in a wheat-infecting isolate of *P. oryzae*. Interestingly, we also identified two novel satellite-like RNAs (ARNA1 and ARNA3) associated with PoOLV1 and PoOLV3, respectively. Characteristics of ARNA1 and ARNA3 are unique and thus, provide a new insight into the diversity of virus-related RNAs in fungi.

2. Results

2.1. Identification of novel mycoviruses and their possible associated RNAs in a wheat isolate of Pyricularia oryzae

During analysis of RNA-seq data obtained from the wheat-infecting *P. oryzae* isolate, Br48 (Pham et al., 2015), abundant transcripts showing homology to RdRP were found. To further characterize the RdRP-like sequences, contigs were constructed from a subset of the reads that were not mapped to the *P. oryzae* genome. The resulting 1,864 contigs longer than 1,000 nucleotides (nt) were subjected to BLAST searches against public databases. Consequently, three distinct contigs were found to show significant similarities with RdRP sequences of plant ourmia viruses and ourmia-like mycoviruses, which we named Pyricularia oryzae ourmia-like virus 1 to 3 (PoOLV1-3). We also performed BLAST analysis of the top 50 contigs (longer than 200 nt) ranked by the abundance of mapped reads. Interestingly, two of the 50 contigs were found to have 5′ terminal sequences (25 and 255 nt) identical to ones in the 5′ and 3’ terminal regions of PoOLV1 and PoOLV3, respectively (Fig. 1A). We tentatively named them PoOLV1- and PoOLV3-associated RNAs (hereafter referred to as ARNA1 and ARNA3). Based on the data of directed RNA-seq, ARNA1 and ARNA3 are apparently single-stranded RNAs of approximately 0.6 and 0.5 Kb.

Northern analysis was performed to confirm the presence of these virus-related sequences in Br48. Two fluorescein-labeled oligonucleotides, FI-VA1 and FI-VA3, which are complementary to the shared sequences between PoOLV1 and ARNA1, and between PoOLV3 and ARNA3, were synthesized and used as probes (Fig. 1A). To detect PoOLV2, a fluorescein-labeled PCR fragment of approximately 150 bp in RdRP (FI–V2) was used as a probe. When probed with FI-VA1, two major bands were detected at approximately 2.5 and 0.6 Kb, likely corresponding to PoOLV1 and ARNA1, in addition to other minor bands below 1.0 Kb (Fig. 1B). Similarly, the FI-VA3 probe detected two major bands at approximately 2.6 and 0.5 Kb, possibly corresponding to PoOLV3 and ARNA3. By probing with FI-V2, a major band around 1.6 Kb and several minor bands below it were detected. These results were mostly consistent with the contig lengths of PoOLVs and their associated RNAs. S1 nuclease treatment indicated that all PoOLVs and ARNAs were single stranded RNAs (data not shown).

We performed local BLAST searches of PoOLV and ARNA sequences against our *de novo* assembled Br48 genome as well as against Illumina HiSeq reads of Br48 genomic DNA to seek a possibility of endogenization of PoOLVs and ARNAs. However, the length of the longest perfect match found was only 19 nt, and the BLAST hit sequences were not clustered in the genome. Thus, PoOLVs and ARNAs were not endogenized in the Br48 genome.

2.2. 5′ and 3’ RLM-RACE of PoOLVs and their associated RNAs

To determine the terminal sequences of PoOLVs and their associated RNAs, we performed RNA ligase-mediated rapid amplification of cDNA ends (RLM-RACE). The sequencing of the resulting RACE fragments indicated that the sizes of their full length genome were as follows; PoOLV1, 2,528 nt; PoOLV2, 1,671 nt; PoOLV3, 2,557 nt; ARNA1, 639 nt; ARNA3, 514 nt. With regard to the 3’ terminus of PoOLV2, various RACE fragments of different lengths with base substitutions and deletions were obtained. This may result in a broad PoOLV2 band in northern analysis (Fig. 1B).

Each of the PoOLVs possesses a single ORF encoding RdRP. The sizes of their putative ORFs are 1,995 nt (PoOLV1), 1,101 nt (PoOLV2), and 1,959 nt (PoOLV3). ARNA1 and ARNA3 also have one and two putative short ORFs, respectively, on the sense strand. The predicted products of ARNA1 ORF1 and, ARNA3 ORF1 and ORF2 (51 aa, 44 aa, and 53 aa, respectively) had no significant similarity with known protein sequences in the public databases.

Previous studies indicated the presence of a stable stem-loop structure in the 5′ and/or 3′ non coding regions (NCRs) of plant ourmiaviruses, OuMV, EpCV, and CsCV (Donaire et al., 2016). In addition, BOLV, an ourmia-like virus in the fungus *Botrytis cinerea*, also possessed stretches of 28 and 50 nt sequences that could form a slightly less stable stem-loop structure involving the 5′ and 3′ NCRs, respectively (Donaire et al., 2016). The predicted secondary structure of PoOLV1 RNA indicated that the first 50 nt in the 5′ NCR are folded into two stable stem-loop structures and the latter was shared with ARNA1 (Fig. 2). The last 31 nt of the 3′ NCR of PoOLV1 RNA could also form a stable stem-loop structure (Fig. 2). Similarly, a stable stem-loop structure was predicted involving the other terminal regions of PoOLV2 and ARNA1 (Fig. 2). In contrast, no such stable stem-loop structure was found in either the 5′ or 3’ NCR of PoOLV3 RNA and ARNA3.

2.3. RdRP-based phylogenetic relationship of PoOLVs to ourmiaviruses, ourmia-like viruses, narnaviruses, and mitoviruses

To examine the phylogenetic relationship of MoOLVs to known related viruses, a phylogenetic tree was constructed using the neighbor joining method based on RdRP amino acid sequences from three plant ourmiaviruses, nine fungal ourmia-like viruses, two yeast narnaviruses, twelve invertebrate narna-like viruses, eleven mitoviruses, and one levivirus as an outgroup. The results indicated that there were four major clades supported by high bootstrap values in the phylogenetic tree, *Mitovirus*, *Narnavirus*, *Ourmiavirus*, and Ourmycovirus as previously proposed by Hrabakove et al. (2017). Interestingly, the majority of the invertebrate narna-like viruses were clustered with plant ourmiaviruses, and a few of them were with yeast narnaviruses and fungal mitoviruses but none were with fungal ourmia-like viruses (Fig. 3). Thus, Ourmycovirus might be specific to fungi. High similarity between the RdRP sequences of the invertebrate viruses and plant ourmiaviruses suggested that plant ourmiaviruses have acquired an RdRP gene from their relatives.

PoOLVs were all grouped into Ourmycovirus. Members of Ourmycovirus can be divided into two well-supported sub-clades typified by Sclerotinia sclerotiorum ourmia-like virus (SsOLV) 1 and 2, respectively (Fig. 3). PoOLV1 clustered with SsOLV2, and PoOLV2 and PoOLV3 grouped with SsOLV1. MOLV1, an ourmia-like virus identified in a rice-infecting *P. oryzae* isolate, is a member of the SsOLV1 subclade. However, PoOLV2 and PoOLV3 are relatively distantly related to MOLV1 in the subclade, suggesting the presence of diverse ourmia-like viruses in the *P. oryzae* natural population.

2.4. Association of ARNA1 and ARNA3 with PoOLVs in field isolates of P. oryzae and a mutant of MoAGO2 (Δago2)

While virus-associated RNAs such as satellite RNAs are usually

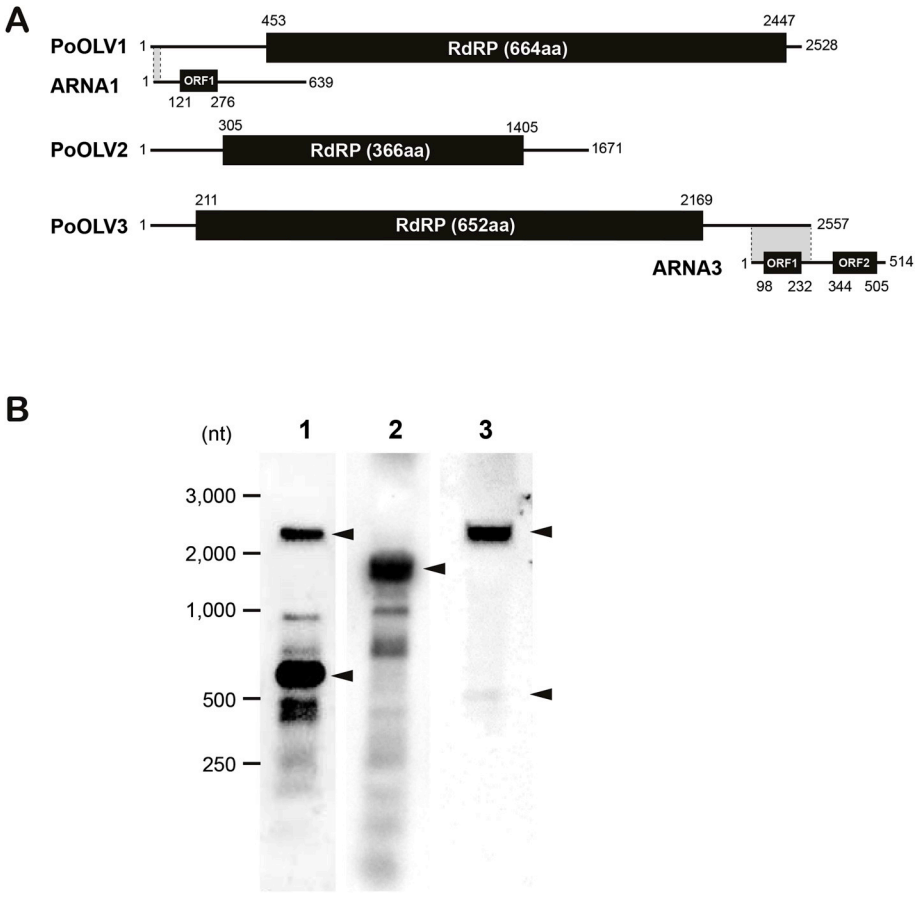

Fig. 1. Identification of three ourmia-like viruses and their associated RNAs in *P. oryzae*. (A) Schematic representation of the genomic organization of viral genomic RNAs and their associated RNAs. The openreading frames are shaded in black. Grey shading indicates regions in which a helper virus and an associated RNA share the sequence. The sequences of PoOLVs and ARNAs were deposited to the DDBJ/EMBL/GenBank databases under the accession numbers, LC413501 (PoOLV1), LC413502 (PoOLV2), LC413503 (PoOLV3), LC413504 (ARNA1), and LC413505 (ARNA3). (B) Northern blot hybridization analysis of PoOLVs and their associated RNAs. Two fluorescein-labeled oligonucleotides complementary to the sequences shared between PoOLV1 and ARNA1, and between PoOLV3 and ARNA3, were synthesized and used to probe the corresponding elements. To probe PoOLV2, a DNA fragment of approximately 150 bp of RdRP was fluorescein-labeled and used. The position of the RNA ladder is shown on the left. Arrows on the right indicate positions of PoOLVs and associated RNAs estimated from their contig sizes.

encapsidated, members of Ourmycovirus are believed to have no capsid structure, making it impossible to verify the association of ARNAs with PoOLVs by capsid isolation. Thus, we first tried to examine the association between ARNAs and PoOLVs by determining the levels of PoOLVs and ARNAs in field isolates of *Pyricularia* using RT-qPCR analysis. Since the original host isolate, Br48 belongs to the TELE groups (named after *Triticum*, *Eleusine*, *Lolium*, and *Eragrostis*) in *P. oryzae* (Hirata et al., 2007), ten isolates from the TELE groups, in addition to three isolates from other *P. oryzae* groups and one *P. grisea* isolate (Dig41), were used in the analysis (Table 1). PoOLV1 was detectable in all of the *Pyricularia* isolates examined (Fig. 4A). However, the level of PoOLV1 accumulation in the isolates were generally much lower than those in Br48. Nevertheless, the prevalence of PoOLV1 in the diverse *Pyricularia* isolates from different geographical and host origins implies that this virus might be vertically transmitted and maintained during the evolution of *Pyricularia* species. It is also to be noted that the levels of PoOLV1 were well-correlated with those of ARNA1 ($R^2 = 1.00$) in the *Pyricularia* isolates, supporting the association of ARNA1 with PoOLV1 (Fig. 4A).

With regard to PoOLV2, the levels of accumulation were mostly very low in the isolate tested, except Br48. PoOLV2 was sporadically detected in *P. oryzae* isolates even within the TELE groups. Notably, PoOLV2 was present, albeit at a very low level, in the *P. grisea* isolate Dig41. Thus, the distribution of PoOLV2 was not always consistent with the phylogenetic relationship of the host fungi (Fig. 4B).

PoOLV3 was detectable only in the TELE groups at highly variable levels (Fig. 4C). While some isolates of the TELE group such as AK1 and LW3, were not infected with PoOLV3 at detectable levels, the level of PoOLV3 accumulation was comparable to that in Br48 in a wheat-infecting strain (Br7). Similar to the case with PoOLV1 and ARNA1, the accumulation levels of PoOLV3 in the isolates were significantly correlated with those of ARNA3 ($R^2 = 0.94$), suggesting that ARNA3 multiplication was associated with PoOLV3.

We next examined the accumulation levels of PoOLVs and ARNAs in a deletion mutant of MoAGO2 (Δago2). We previously reported that MoAGO2 negatively affects the RNAi pathway through competition for sRNA binding against MoAGO1 (Nguyen et al., 2018). Thus, in Δago2, the accumulation levels of PoOLV1 and PoOLV2 were drastically decreased to less than 1/1000 compared to those in the wild-type strain (Nguyen et al., 2018). RT-qPCR analysis revealed that ARNA1 accumulation was also drastically decreased in Δago2 to a level similar to PoOLV1, again supporting the association of ARNA1 replication with PoOLV1 (Fig. 4D). The level of PoOLV3 accumulation was also reduced in Δago2 but only by less than 90% (Fig. 4D). Similarly, the level of ARNA3 accumulation in Δago2 showed only an approximately 60% reduction compared to that of the wild-type strain. These observations were consistent with the hypothesis that ARNA3 replication is associated with PoOLV3.

2.5. Transmission of PoOLVs and ARNAs to sexual and asexual progenies

The efficacy of transmission of PoOLVs and ARNAs to progenies through sexual and asexual spores was examined. A complete set of eight isolates were obtained from a single ascus produced by a cross between the Br48 and GFSI1-7-2 strains. The GFSI1-7-2 strain is infected with PoOLV1 at a low level but not with PoOLV2 or PoOLV3 (Fig. 4A–C). Seven isolates were also obtained from individual conidia of the Br48 strain.

RT-qPCR revealed that none of the virus-related elements were detected in the sexual progenies even though both mating parents possess PoOLV1 and ARNA1 (Fig. 5A), suggesting a possible defense mechanism to protect sexual progeny from virus infection in *P. oryzae*. In contrast, every virus-related element was detectable in the asexual progeny. However, compared to the parent strain, the average RNA

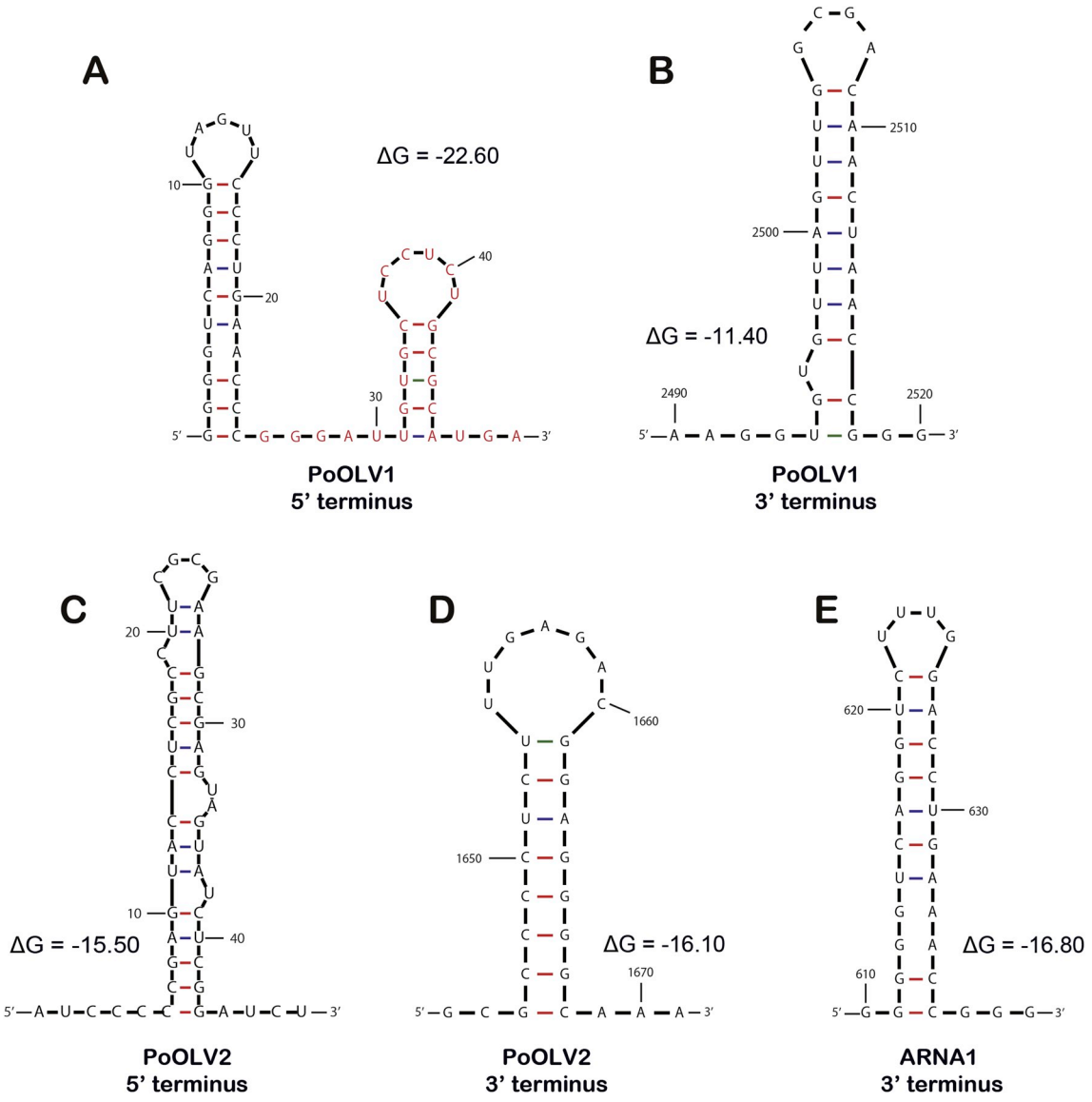

Fig. 2. PoOLV1, PoOLV2, and ARNA1 possess potential stem-loop structures at their 5′ and 3′ terminal regions. Predicted secondary structures of the 5'- (A and C) and 3'- (B, D, and E) terminal sequences of PoOLV1, PoOLV2, and ARNA1, respectively, and their ΔG values (kcal/mol) were obtained using Mfold (http://unafold.rna.albany.edu/). The nucleotides shown in red in A represent sequences conserved between PoOLV1 and ARNA1.

levels of PoOLV1, PoOLV3, and ARNA1 were rather higher while those of PoOLV2 and ARNA3 were lower (0.37 and 0.20 fold, respectively) in the asexual progeny. The RNA accumulation levels of a virus-related element also showed, in some cases, more than 10 times difference among the individual asexual progenies (Fig. 5B and C). Nevertheless, the difference in RNA accumulation between the virus-related elements, as indicated by different letters in Fig. 5A, was statistically significant. This implies that the efficacy of transmission to asexual progeny and/or that of virus multiplication after transmission to a conidium was significantly different among the elements (Fig. 5A).

Then, correlation of PoOLV1 and ARNA1 as well as PoOLV3 and ARNA3 in the asexual progenies was assessed. As shown in Fig. 5B, the RNA levels of PoOLV1 and ARNA1 were well-correlated at a statistically significant level ($R^2 = 0.822$, $P < 0.05$). Interestingly, while the accumulation levels of ARNA3 were considerably decreased in the asexual progenies as mentioned above, they were still correlated with the levels of PoOLV3 RNA ($R^2 = 0.909$), suggesting PoOLV3-dependent ARNA3 replication. The fact that generally low accumulation levels of ARNA3 did not affect the levels of PoOLV3 in the asexual progenies indicated that ARNA3 may not be essential for PoOLV3 replication.

2.6. Gene silencing of PoOLVs by a retrotransposon-based vector

Finally, we tried to silence individual PoOLVs using pSilent-MG, which is a plasmid vector for retrotransposon-induced gene silencing (Vu et al., 2011). In this system, a target sequence inserted into 3' UTR of the retrotransposon MAGGY functions as a trigger of gene silencing. A cDNA fragment (150-300bp) specific to each virus was amplified by PCR and inserted into pSilent-MG. At least 3 independent knock-down (KD) strains were obtained for each PoOLV. We first performed phenotypic assay of the KD strains to assess the potential of PoOLVs as a biocontrol agent. However, no phenotypic differences in growth and pathogenicity were observed between the wild type and any of the virus-KD strains (Fig. S1), indicating that infection of PoOLVs has no effects on the pathogenicity of the host fungus.

Next, to gain insight into the relationship among PoOLVs and ARNAs, their RNA levels were assessed in the PoOLV-KD transformants. Compared to the wild-type strain, the RNA level of ARNA1 was deceased in the PoOLV1-KD strains as expected (Fig. 6A), again indicating PoOLV1-dependent replication of ARNA1.

In the PoOLV2-KD strain, the accumulation level of PoOLV1 did not

change at a statistically significant level but the levels of PoOLV3 and ARNA3 were decreased by approximately 50% in average (Fig. 6A). Similarly, when PoOLV3 was targeted for gene silencing, the accumulation level of PoOLV2, in addition to that of ARNA3, was severely reduced. There results suggested that the replication of PoOLV2 and PoOLV3 could be associated with each other, or it may be caused by mutual off-target effects since PoOLV2 and PoOLV3 were phylogenetically close (Fig. 3).

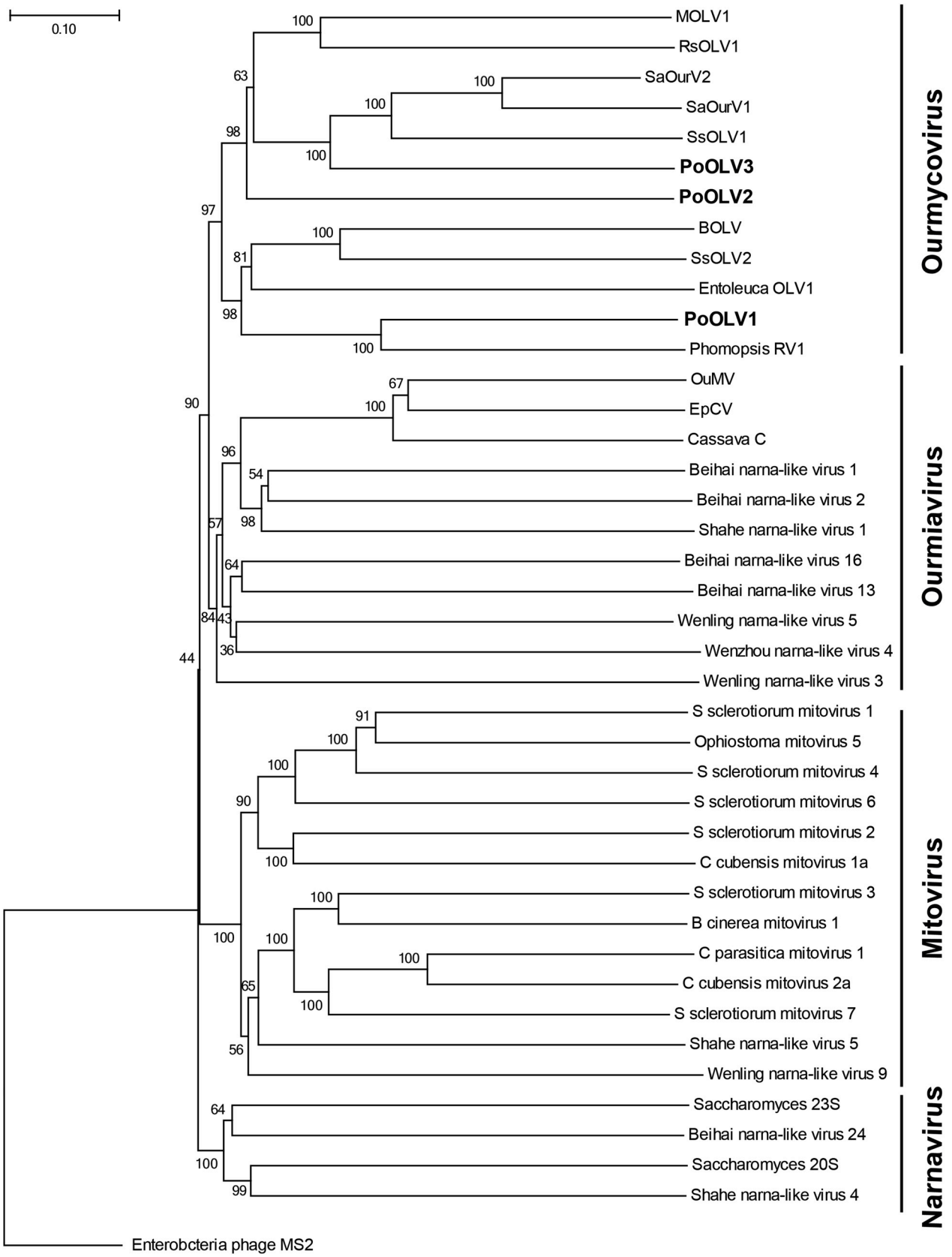

(caption on next page)

Fig. 3. RdRP-based phylogenetic relationship of MoOLVs to ourmiaviruses, ourmia-like viruses, narnaviruses, and mitoviruses. A neighbor-joining tree was constructed by alignment of RdRP sequences from ourmiaviruses, ourmia-like viruses, narnaviruses, and mitoviruses. Enterobcteria phage MS2 was used as outgroup. Bootstrap values are shown from 1000 replicates. Accession numbers of sequences are as follows: Beihai narna-like virus 1 (KX883515), Beihai narna-like virus 2 (KX883512), Beihai narna-like virus 13 (YP_009333241), Beihai narna-like virus 16 (YP_009333152), Beihai narna-like virus 24 (YP_009333245), B cinerea mitovirus 1 (YP_002284334), BOLV (LN827955), Cassava C (YP_003104770), C cubensis mitovirus 1a (AAR01970), C cubensis mitovirus 2a (AAR01973), C parasitica mitovirus 1 (NP_660174), Entoleuca OLV1 (AVD68674), Enterobcteria phage MS2 (P00585), EpCV (YP_002019754), MOLV1 (LT593139), Ophiostoma mitovirus 5 (NP_660180), OuMV (YP_002019757), Phomopsis RV1 (YP_009345044), PoOLV1, PoOLV2, PoOLV3, RsOLV1 (ALD89131), Saccharomyces_20S (NP_660178), Saccharomyces_23S (NP_660177), SaOurV1 (KT598235), SaOurV2 (KT598247), Shahe narna-like virus 1 (KX883553), Shahe narna-like virus 4 (APG77168), Shahe narna-like virus 5 (YP_009336548), S sclerotiorum mitovirus 1 (YP_009121785), S sclerotiorum mitovirus 2 (AEX91879), S sclerotiorum mitovirus 3 (AGC24232), S sclerotiorum mitovirus 4 (AMT92141), S sclerotiorum mitovirus 6 (YP_009009144), S sclerotiorum mitovirus 7 (AHE13866S), sOLV1 (ALD89138), SsOLV2 (ALD89139), Wenling narna-like virus 3 (YP_009337159), Wenling narna-like virus 5 (YP_009337146), Wenling narna-like virus 9 (YP_009337200), Wenzhou narna-like virus 4 (YP_009333318).

Table 1
Pyricularia isolates used in this study.

Isolate	Species	Original host	Locality	Subgroup[a]
Br48	*P. oryzae*	*Triticum aestivum*	Brazil (Mato Grosso do Sul)	TELE3
Br3	*P. oryzae*	*Triticum aestivum*	Brazil (Parana)	TELE3
Br115.7	*P. oryzae*	*Triticum aestivum*	Brazil (Parana)	TELE1
Br118.2	*P. oryzae*	*Triticum aestivum*	Brazil (Parana)	TELE1
Br7	*P. oryzae*	*Triticum aestivum*	Brazil (Parana)	TELE1
Br58	*P. oryzae*	*Avena sativa*	Brazil (Parana)	TELE1
LW3	*P. oryzae*	*Lolium perenne*	Japan (Yamanashi)	TELE1
AK1	*P. oryzae*	*Lolium perenne*	Japan (Akita)	TELE1
TP2	*P. oryzae*	*Lolium perenne*	Japan (Tochigi)	TELE1
MZ5-1-6	*P. oryzae*	*Eleusine coracana*	Japan (Miyazaki)	TELE1
GFSI1-7-2	*P. oryzae*	*Setaria italica*	Japan (Gifu)	SP
Ina168	*P. oryzae*	*Oryza sativa*	Japan (Aichi)	Os2
Guy11	*P. oryzae*	*Oryza sativa*	Guiana (Combi)	Os1
Dig41	*P. grisea*	*Digitaria sanguinalis*	Japan (Hyogo)	Dssh4

[a] Based on Hirata et al. (2007).

In addition, during screening for PoOLV3-KD strains, we obtained a spheroplast-regenerant (KD3_2_7) possessing ARNA1 at a very low level (approximately 1/1000 relative to the wild type). RT-qPCR analysis revealed that the level of PoOLV1 in the regenerant was comparable to that in the wild type (Fig. 6B), indicating that ARNA1 is not essential for PoOLV1 replication.

3. Discussion

Members of the family *Narnaviridae* are characterized by their capsidless nature and simple undivided genomes comprising a 2–3 Kb ssRNA encoding RdRP as its sole product. *Narnaviridae* has two genera: *Narnavirus* and *Mitovirus*. Plant-infecting, multi-segmented ourmiaviruses are also related to *Narnaviridae* since their RdRPs are phylogenetically close to those of *Narnavirus*. An increasing number of ourmia-like viruses have been detected from diverse filamentous fungi, for which the genus Ourmycovirus was proposed (Hrabakove et al., 2017). However, little is known about their biological characteristics. This study describes three novel ourmycoviruses and associated subviral RNAs from *P. oryzae* and provides insights into their molecular and evolutionary biology.

Where ourmycoviruses replicate in infected cells is one of the important unanswered questions. Just like naraviruses and mitoviruses, ourmycoviruses are thought to have a simple undivided genome. While naraviruses use the universal genetic code and replicate in the cytosol, mitoviruses predominantly adopt the fungal mitochondrial genetic code that uses UGA as a tryptophan codon, and thus, replicate in mitochondria (Nibert, 2017). The RdRP amino acid sequences of PoOLV1 to 3 contain 10, 6 and 17 tryptophan residues, respectively. However, the standard UGG codon is used for every tryptophan residue, supporting the hypothesis that PoOLVs replicate in the cytosol. In addition, accumulation levels of PoOLVs and ARNAs were significantly affected by the mutation of MoAGO2 and Dicer (Nguyen et al., 2018, Fig. 4D), suggesting that their replication was potentially suppressed by RNA silencing that is believed to operate in the cytoplasm. Taken together, our data favors the cytoplasmic replication of PoOLVs and ARNAs.

PoOLV2 possesses an extraordinary short RdRP consisting of only 366 amino acid residues. The gene silencing experiments revealed that the accumulation level of PoOLV2 was drastically reduced in the PoOLV3-KD strains. Thus, it is possible to assume that PoOLV2 replicated using PoOLV3 RdRP. However, since PoOLV2 was detectable in *Pyricularia* strains that were not infected with PoOLV3 (Fig. 4B and C), PoOLV2 should also be able to use a helper virus (HV) other than PoOLV3 if it is not an autonomous virus.

While members of the family *Narnaviridae* are characterized by simple genome organization, Ophiostoma novo-ulmi mitovirus 3a (OnuMV3a) and OnuMV3b, members of *Narnaviridae*, were shown to possess a virus-associated RNA in *Sclerotinia homoeocarpa* (Deng and Boland, 2004; Wu et al., 2010). Virus-associated RNA can be satellite RNA, satellite virus, and defective (D) RNA. Satellite RNAs and satellite viruses share a common feature in that they generally have little or no sequence homology to their HVs but differ in that the latter typically carry a gene encoding their own capsid protein. Instead, small linear satellite RNAs of plants usually have a high proportion of base-pairing in their structures that could contribute to their protection from RNA silencing (Wang et al., 2004). D-RNA is a defective form of HV, and thus, its sequence is nearly or completely identical to a portion of HV. These elements are generally not essential for the infection cycle of HVs. However, they could attenuate or enhance the pathogenicity of HVs, and, in some cases, play a role in virus transmission and movement (Simon et al., 2004; Taliansky et al., 2000).

Alternatively, virus-associated RNA might represent as-yet unidentified genomic RNA of a multipartite virus. Genomic RNAs of a multipartite virus usually share common sequences at their 5′ and/or 3’ ends for replication and encapsidation. Unlike the sub-viral elements mentioned above, viral genomic RNA is generally required for a normal life cycle of the virus, and is often evolutionarily conserved among related viruses.

In this study, two novel virus associated RNAs, ARNA1 and ARNA3 were identified in *P. oryzae*. ARNA1 and ARNA3 possess one and two small ORFs, respectively, and neither of them form highly base-paired secondary structures. ARNA1 shares a stretch of 25 nt with PoOLV1 at the 5′ terminal region, while the 5′ half of ARNA3 (255 nt) was identical to the 3’ end of PoOLV3. Thus, the molecular mechanism of association with HVs seems to be non-conserved between ARNA1 and ARNA3. Based on the results in Figs. 5A and 6B, both ARNA1 and ARNA3 were not essential for the replication of HVs since the accumulation levels of their HVs were comparable to those in the wild-type strain even in asexual progenies and spheroplast-regenerants possessing ARNA3 and ARNA1, respectively, at very low levels.

These characteristics of ARNA1 and ARNA3 do not fully meet any criteria of known virus associated RNAs. Possible related elements are satellite RNAs of turnip crinkle virus (TCV) (Simon and Howell, 1986; Cascone et al., 1990) and Panicum mosaic virus (PMV) (Pyle et al.,

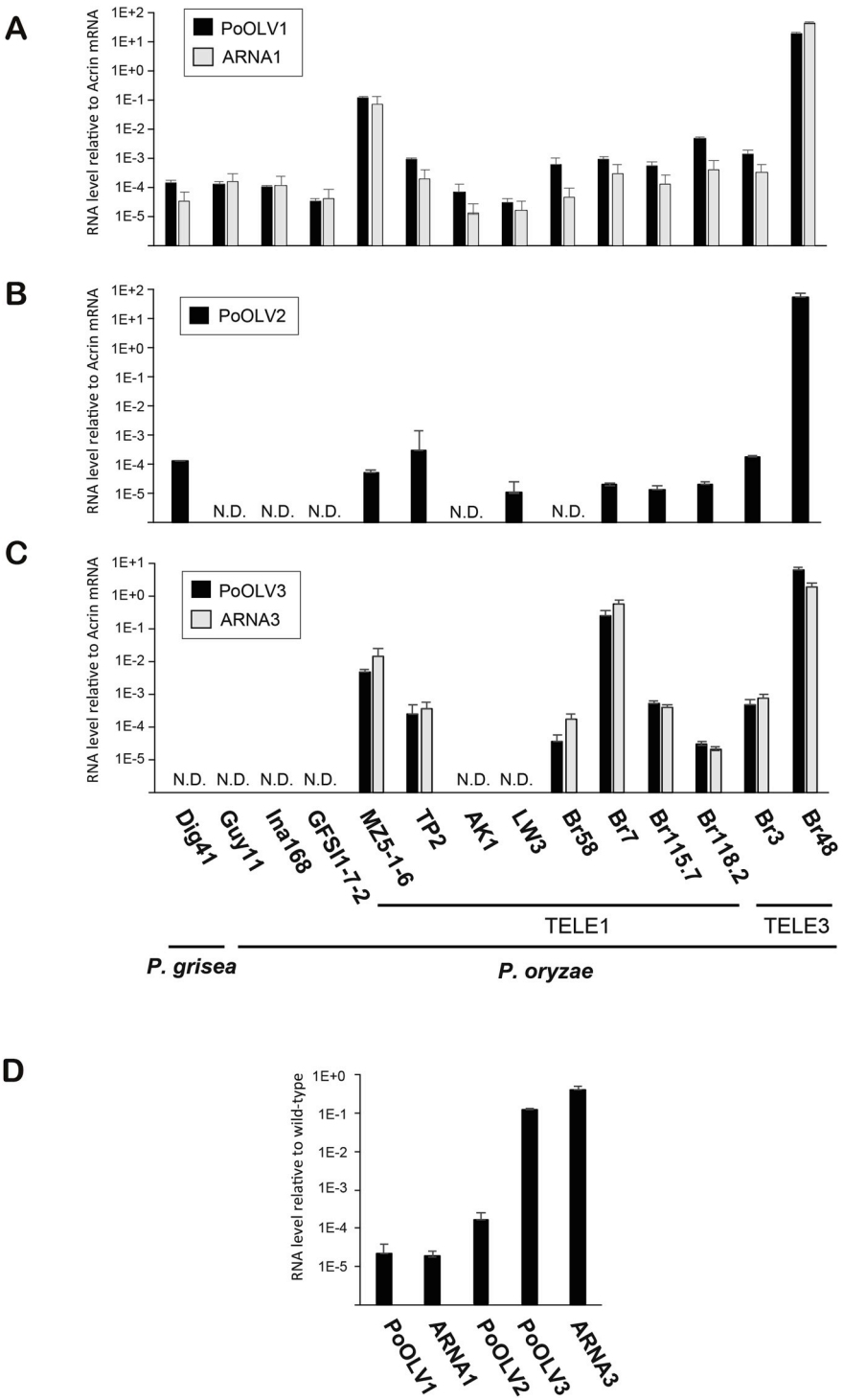

Fig. 4. ARNA1 and ARNA3 are associated with PoOLV1 and PoOLV3, respectively. RT-qPCR analysis of PoOLV1 and ARNA1 (A), PoOLV2 (B), and PoOLV3 and ARNA3 (C) in 14 Pyricularia isolates from various host plants (Table 1). TELE1 and TELE3 are subgroups of *P. oryzae,* based on multilocus phylogenetic analysis (Hirata et al., 2007). The actin gene (MGG_03982) was used to normalize the data. (D) RT-qPCR analysis of PoOLVs and ARNAs in a deletion mutant of MoAGO2. The actin gene was used as an internal control. RNA levels relative to the wild-type strain are represented.

2017). The 3′ half (166 nt) of satellite RNA C was nearly identical to two regions at the 3′ end of the TCV genome. In addition, satellite RNAs C, D, and F shared an identical 7 nt motif with TCV RNA at their 3′ ends (Simon and Howell, 1986). Similarly, 3′ terminal region (nearly 100 nt) of satC showed high sequence similarity (88%) to the 3' end of PMV (Pyle et al., 2017). In addition, satC possessed a small putative ORF of 71 amino acids in the complementary strand. Their patterns of sequence homology between HVs and satellite RNAs were similar to those found between PoOLVs and ARNAs.

Alternatively, ARNA3 might have arisen as a consequence of recombination between D-RNA of PoOLV3 and satellite -like RNA species in *P. oryzae*. Recombination of virus-related RNA has often been reported in animals, plants, and fungi (Simon and Howell, 1986; White and Morris, 1994; Zhang and Nuss, 2008). Recently, the involvement of

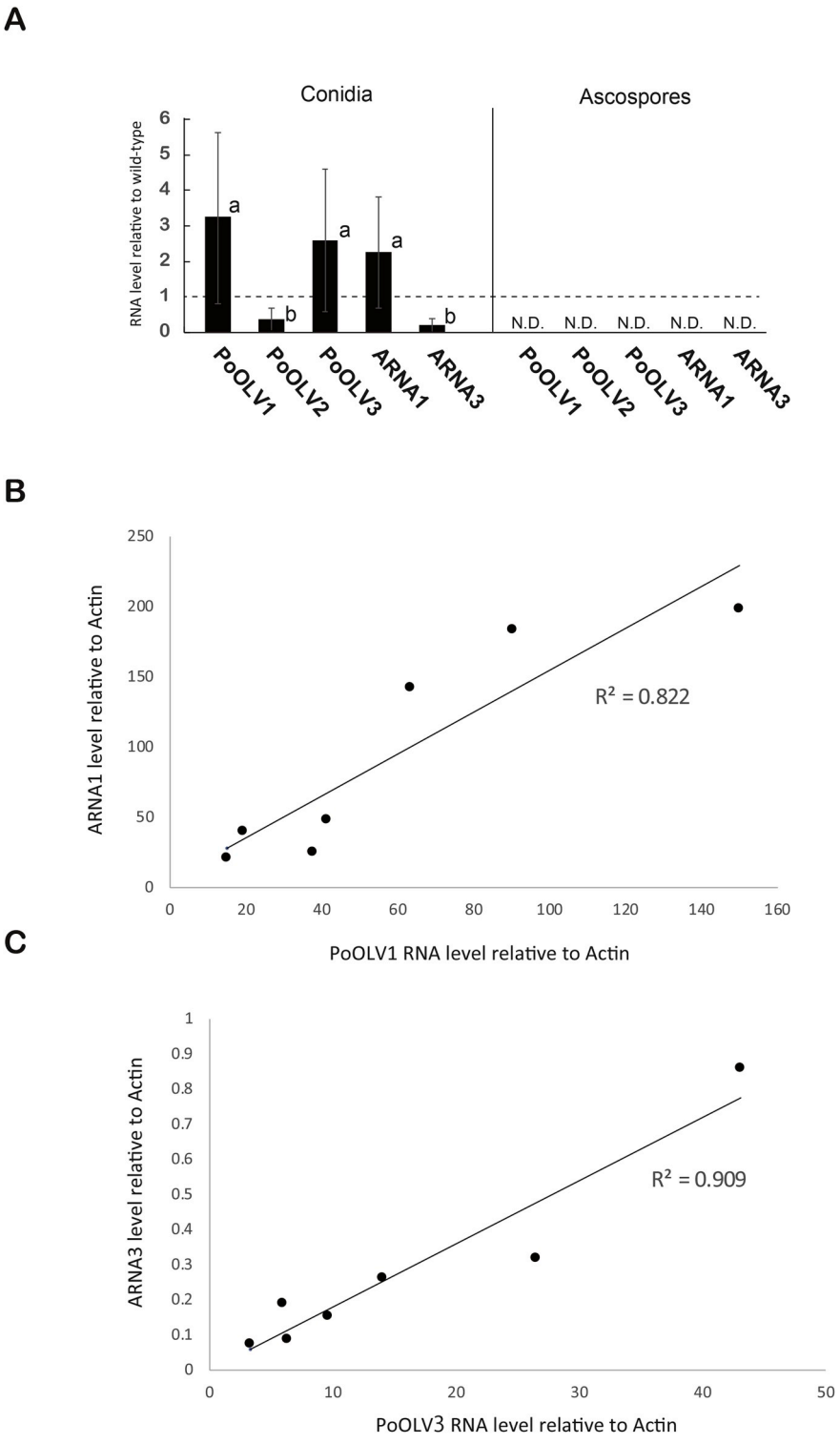

Fig. 5. Transmission of PoOLVs and ARNA3s to sexual and asexual progenies. (A) RT-qPCR analysis of PoOLVs and ARNAs in sexual (Ascospores) and asexual (Conidia) progenies. Seven and eight progeny strains derived from a single conidium and ascospore, respectively, were used in the analysis. The actin gene (MGG_03982) was used to normalize the data. RNA levels relative to the wild-type strain are represented. (B) Correlation between PoOLV1 and ARNA1 in each conidium progeny strain. (C) Correlation between PoOLV3 and ARNA3 in each conidium progeny strain.

RNAi components in the production of D-RNA and in RNA recombination has been demonstrated in the fungus *Cryphonectria parasitica* (Zhang and Nuss, 2008). These results suggest that a new RNA molecule can be generated by recombination among viruses, D-RNAs and satellite RNAs in the host cell. ARNAs might represent one such molecule type.

4. Materials and methods

4.1. Fungal strains and growth conditions

The original hosts and locality of fungal strains used to survey PoOLVs and ARNAs were given in Table 1. The isolates were purified by

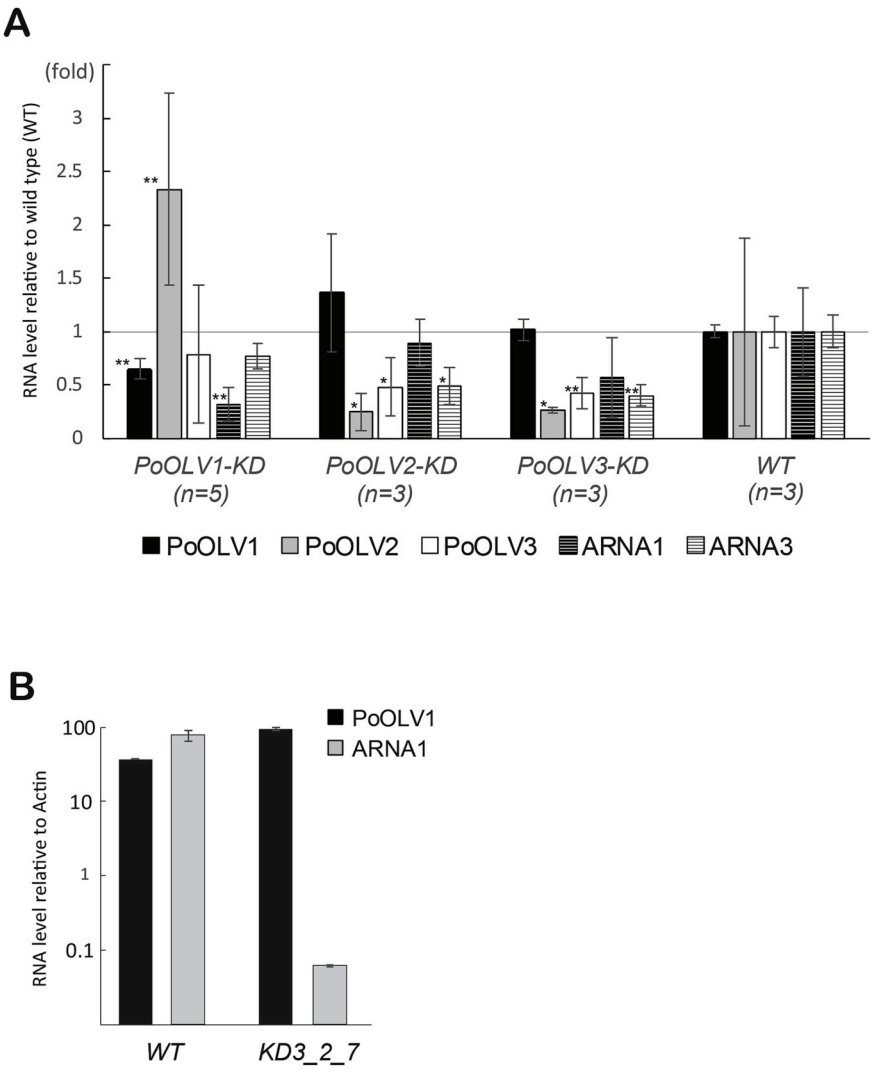

Fig. 6. RNA accumulation levels of PoOLVs and ARNAs in knock-down (KD) strains of each PoOLV. (A) RNA quantity of each element was assessed by RT-qPCR analysis using the actin gene (MGG_03982) as an internal control. The number of KD or wild-type (WT) strains used in the analysis is indicated under the graph. Asterisks indicate significant difference between WT and KD strains (T test; *$p < 0.05$ and **$p < 0.01$). Bars indicate SE. (B) RNA accumulation levels of PoOLV1 and ARNA1 in WT and KD3_2_7 strains. The actin gene was used as an internal control. Bars indicate SE.

monoconidial isolation and maintained on PDA media for short-time storage or on sterilized barley seeds for long-time storage as described previously (Nakayashiki et al., 1999). Preparation of fungal conidia and mating of *P. oryzae* strains were performed as described previously (Murakami et al., 2000).

4.2. Bioinformatics

The RNA-seq data that we previously obtained from mycelia and germination tubes of *P. oryzae* strain Br48 (DRX019597, DRX019601, DRX019596, DRX019600), were mapped to the published *M. oryzae* (*P. oryzae*) genome of the laboratory strain 70-15 as well as to the Br48 genome contigs. The resulting unmapped reads were collected, and then *de novo* assembled using CLC Genomics Workbench software (version 11.0.1) with a minimum contig length of 200 nt. To search for viral sequences, contigs larger than 1,000 nt were subjected to BLAST analysis against the NCBI database (Altschul et al., 1997) at the nucleotide and protein levels. In addition, we performed the primary sequence analysis of the top 50 contigs ranked by the abundance of mapped reads without the size exclusion of 1,000 nt.

Amino acid sequences of viral RdRPs were aligned using the CLUSTAL W program at DDBJ (https://www.ddbj.nig.ac.jp/) under default parameters. Phylogenetic relationships were inferred by the neighbor-joining method using bootstrap phylogeny tests with 1000 replication. A phylogenetic tree was constructed using MEGA 6.0 (Tamura et al., 2013).

Potential secondary structures involving the 5′ and 3′ terminal regions were examined, and their free energies (ΔG) were estimated, using mfold (http://mfold.rna.albany.edu/; Zuker, 2003) with default parameters.

4.3. Northern blot and RT-qPCR analyses

For RNA extraction, fungal mycelia were grown in CM liquid broth (0.3% Casamino acids, 0.3% yeast extract, 0.5% sucrose) at 26 °C for 5 days on an orbital shaker (120 rpm). The mycelial mass was collected and ground to a fine powder in liquid nitrogen with a mortar and pestle. Total RNA was isolated from frozen mycelial powder using Sepasol RNA I Super G (Nacalai Tesque, Japan).

For northern analysis, 20–30 μg of total RNA was separated on a 1.2% (w/v) denaturing agarose gel in 1 x MOPS (20 mM morpholinopropanesulfonic acid, 2 mM sodium acetate, 1 mM EDTA, pH 7.0) containing 4% formaldehyde solution for 2 h at 80 V. Before loading, RNA preparations were mixed with 2 vol of freshly prepared loading

buffer (80% formamide, 1.6 x MOPS, 2% glycerine, 0.01% bromophenol blue) and denatured for 10 min at 68 °C. RNA was transferred to Hybond-NX (GE Healthcare, England) by capillary transfer with 6x SSC overnight. Nucleic acids were fixed by UV crosslinking (70 mJ/cm^2). Two fluorescein-labeled oligonucleotides, FI-VA1 (5′-tagttttccagacccgttagggcgagg-3′) and FI-VA3 (5′-atgcgcagaggagcacaatcccggtttc-3′) were synthesized. Since the sequences of FI-VA1 and FI-VA3 were complementary to the shared sequences between PoOLV1 and ARNA1, and between PoOLV3 and ARNA3, respectively, these probes were used to detect the corresponding elements. To detect PoOLV2, a fluorescein-12-dUTP-labeled DNA fragment of the RdRP domain was amplified by PCR with a pair of primers (5′-tctcggcatcacgagaggta-3′, 5′-tcagatgacgaaccagtcgc-3′) and used as a probe. Hybridization was performed in PerfectHyb™ plus hybridization buffer (Sigma-Aldrich, St. Louis) at 50 °C overnight. Chemiluminescent signals were detected with anti-fluorescein-AP conjugate (Roche Applied Science, Switzerland) and CDP-star (GE Healthcare) using a ChemiDoc Touch imager (Bio-Rad, Hercules).

For RT-qPCR analysis, 1 μg of total RNA was subjected to cDNA synthesis using the ReverTra Ace qPCR RT Master Mix with gDNA Remover kit (Toyobo, Japan). RT-qPCR assays were carried out with FastStart SYBR Green Master (Roche) or GeneAce SYBR qPCR Mix α (Nippon Gene, Japan). Pairs of primers used in RT-qPCR were as follows; PoOLV1: 5′-aagggatgttagggccttgc-3′, 5′-acagttagcacccgggaatgacgaa-3′, PoOLV2: 5′-tctcggcatcacgagaggta-3′, 5′-tcagatgacgaaccagtcgc-3′, PoOLV3: 5′-ctcagatgagctttcagtcgat-3′, 5′-gaagctttaagggtggagacat-3′, ARNA1: 5′-aaggccttttgtaggctagtcatc-3′, 5′-accaataaaaccctgaataggaag-3′, ARNA3: 5′-gtcctgtcttacgctctagtggtg-3′, 5′-cctacgtctcccttcactagtctc-3′, Actin: 5′-gcggttacacctctctaccac-3′, 5′-agtctggatctcctgctcaaag-3′. The actin gene (MGG_03982) was used as an internal control. Fluorescence from DNA-SYBR Green complex was monitored by a Thermal Cycler Dice Realtime System (Takara Bio, Japan) throughout the PCR ampflication. The level of target mRNA, relative to the mean of the internal control was calculated by the comparative Ct method.

4.4. RNA ligase mediated rapid amplification of cDNA ends (RLM-RACE)

5′ and 3′ RLM-RACEs were performed using components in the NEXTlex small RNA-seq kit (Bioo Scientific, Austin). Briefly, 3′adenylated adapter and 5′ adapter were sequentially ligated to total RNA decapped by treatment with RNA 5′ pyrophosphohydrolase (New England Biolabs, Massachusetts). cDNA was synthesized using RT primer (5′-gccttggcacccgagaattcca-3′) and Superscript III (Thermo Fisher Scientific, Massachusetts). To obtain 5′ and 3′ end fragments of PoOLVs and ARNAs, PCR amplification was performed with an element specific primer and RT primer or Nextflex-univ primer (5′-gttcagagttctacagtccgac-3′) using the adapter attached cDNA as a template. In some cases, two-round PCR was carried out after designing nested primers. Amplified cDNA fragments were cloned into pBluescript and subjected to Sanger DNA sequencing.

4.5. Retrotransposon-induced gene silencing

To knock-down PoOLVs, the retrotransposon-based gene silencing vector, pSilent-MG (Vu et al., 2011) was used. cDNA fragments of PoOLVs were amplified by PCR using the following sets of primers; PoOLV1: 5′-ttggatccgacgaagaggttgttctcatt-3′, 5′-atggatcctagccacgcattcctttaactt-3′, PoOLV2: 5′-cgcggatcctctcggcatcacgagaggta-3′, 5′-cgcggatcctcagatgacgaaccagtc-3′, PoOLV3: 5′-cgcagatctctcagatgagctttcagtcg-3′, 5′-cgcagatctgaagctttaagggtggagac-3′. The amplified DNA fragments were digested with *Bgl*II or *Bam*HI, and inserted into the *Bgl*II site of pSilent-MG. The resulting constructs were introduced into the Br48 strain by PEG-mediated transformation as described previously (Nakayashiki et al., 1999). Geneticine-resistant transformants were screened for knock-down of a target virus by RT-qPCR.

Acknowledgments

This work was supported by a Grant-in-Aid for Scientific Research (A) and (B) from the Japan Society for the Promotion of Science (#25252011 and #25292028).

Appendix A. Supplementary data

Supplementary data to this article can be found online at https://doi.org/10.1016/j.virol.2019.05.015.

References

Ai, Y.P., Zhong, J., Chen, C.Y., Zhu, H.J., Gao, B.D., 2016. A novel single-stranded RNA virus isolated from the rice-pathogenic fungus *Magnaporthe oryzae* with similarity to members of the family Tombusviridae. Arch. Virol. 161, 725–729.
Altschul, S., Madden, T., Schaffer, A., Zhang, J., Zhang, Z., Miller, W., Dj, L., 1997. Gapped BLAST and PSI- BLAST: a new generation of protein database search programs. Nucleic Acids Res. 25, 3389–3402.
Bruenn, J.A., Warner, B.E., Yerramsetty, P., 2015. Widespread mitovirus sequences in plant genomes. PeerJ 3, e876.
Cai, G., Myers, K., Fry, W.E., Hillman, B.I., 2012. A member of the virus family Narnaviridae from the plant pathogenic oomycete *Phytophthora infestans*. Arch. Virol. 157, 165–169.
Cascone, P.J., Carpenter, C.D., Li, X.H., Simon, A.E., 1990. Recombination between satellite RNAs of turnip crinkle virus. EMBO J. 9, 1709–1715.
Deng, F., Boland, G.J., 2004. A satellite RNA of Ophiostoma novo- ulmi mitovirus 3a in hypovirulent isolates of *Sclerotinia homoeocarpa*. Phytopathology 94, 917–923.
Donaire, L., Rozas, J., Ayllo´n, M.A., 2016. Molecular characterization of Botrytis ourmia-like virus, a mycovirus close to the plant pathogenic genus Ourmiavirus. Virology 489, 158–164.
Ghabrial, S.A., Suzuki, N., 2009. Viruses of plant pathogenic fungi. Annu. Rev. Phytopathol. 47, 353–384.
Hillman, B.I., Cai, G., 2013. The family narnaviridae: simplest of RNA viruses. Adv. Virus Res. 86, 149–176.
Hirata, K., Kusaba, M., Chuma, I., Osue, J., Nakayashiki, H., Mayama, S., Tosa, Y., 2007. Speciation in *Pyricularia* inferred from multilocus phylogenetic analysis. Mycol. Res. 111, 799–808.
Hong, Y., Cole, T.E., Brasier, C.M., Buck, K.,W., 1998. Evolutionary relationships among putative RNA-dependent RNA polymerases encoded by a mitochondrial virus-like RNA in the Dutch elm disease fungus, *Ophiostoma novo-ulmi*, by other viruses and virus-like RNAs and by the Arabidopsis mitochondrial genome. Virology 246, 158–169.
Hrabáková, L., Koloniuk, I., Petrzik, K., 2017. Phomopsis longicolla RNA virus 1 - novel virus at the edge of myco- and plant viruses. Virology 506, 14–18.
Ikeda, K., Park, P., Nakayashiki, H., 2019. Cell biology in phytopathogenic fungi during host infection: commonalities and differences. J. Gen. Plant Pathol. 85, 163–173.
Illana, A., Marconi, M., Rodriguez-Romero, J., Xu, P., Dalmay, T., Wilkinson, M.D., Ayllon, M.A., Sesma, A., 2017. Molecular characterization of a novel ssRNA ourmia-like virus from the rice blast fungus *Magnaporthe oryzae*. Arch. Virol. 162, 891–895.
Li, C.X., Zhu, J.Z., Gao, B.D., Zhu, H.J., Zhou, Q., Zhong, J., 2019. Characterization of a novel ourmia-like mycovirus infecting *Magnaporthe oryzae* and implications for viral diversity and evolution. Viruses 223.
Lisa, V., Milne, R.G., Accotto, G.P., Boccardo, G., Caciagli, P., Parvizy, R., 1988. Ourmia melon virus, a virus from Iran with novel properties. Ann. Appl. Biol. 112, 291–302.
Maejima, K., Himeno, M., Komatsu, K., Kagiwada, S., Yamaji, Y., Hashimoto, H., Namba, S., 2008. Complete nucleotide sequence of a new double-stranded RNA virus from the rice blast fungus, *Magnaporthe oryzae*. Arch. Virol. 153, 389–391.
Mu, F., Xie, J., Cheng, S., You, M.P., Barbetti, M.J., Jia, J., Wang, Q., Cheng, J., Fu, Y., Chen, T., Jiang, D., 2018. Virome characterization of a collection of *Sclerotinia sclerotiorum* from Australia. Front. Microbiol. 8, 2540.
Murakami, J., Tosa, Y., Kataoka, T., Tomita, R., Kawasaki, J., Chuma, I., Sesumi, Y., Kusaba, M., Nakayashiki, H., Mayama, S., 2000. Analysis of host species specificity of *Magnaporthe grisea* toward wheat using a genetic cross between isolates from wheat and foxtail milliet. Phytopathology 90, 1060–1067.
Nakayashiki, H., Kiyotomi, K., Tosa, Y., Mayama, S., 1999. Transposition of the retrotransposon MAGGY in heterologous species of filamentous fungi. Genetics 153, 693–703.
Nguyen, Q., Iritani, A., Ohkita, S., Vu, B.V., Yokoya, K., Matsubara, A., Ikeda, K.I., Suzuki, N., Nakayashiki, H., 2018. A fungal Argonaute interferes with RNA interference. Nucleic Acids Res. 46, 2495–2508.
Nibert, M.L., 2017. Mitovirus UGA(Trp) codon usage parallels that of host mitochondria. Virology 507, 96–100.
Pyle, J.D., Monis, J., Scholthof, K.B., 2017. Complete nucleotide sequences and virion particle association of two satellite RNAs of panicum mosaic virus. Virus Res. 240, 87–93.
Pham, K.T., Inoue, Y., Vu, B.V., Nguyen, H.H., Nakayashiki, T., Ikeda, K., Nakayashiki, H., 2015. MoSET1 (histone H3K4 methyltransferase in *Magnaporthe oryzae*) regulates global gene expression during infection-related morphogenesis. PLoS Genet. 11, e1005385.
Polashock, J.J., Hillman, B.I., 1994. A small mitochondrial double-stranded (ds) RNA element associated with a hypovirulent strain of the chestnut blight fungus and

ancestrally related to yeast cytoplasmic T and W dsRNAs. Proc. Natl. Acad. Sci. U.S.A. 91, 8680–8684.
Rastgou, M., Habibi, M.K., Izadpanah, K., Masenga, V., Milne, R.G., Wolf, Y.I., Koonin, E.V., Turina, M., 2009. Molecular characterization of the plant virus genus Ourmiavirus and evidence of inter-kingdom reassortment of viral genome segments as its possible route of origin. J. Gen. Virol. 90, 2525–2535.
Shi, M., Lin, X.D., Tian, J.H., Chen, L.J., Chen, X., Li, C.X., Qin, X.C., Li, J., Cao, J.P., Eden, J.S., Buchmann, J., Wang, W., Xu, J., Holmes, E.C., Zhang, Y.Z., 2016. Redefining the invertebrate RNA virosphere. Nature 540, 539–543.
Simon, A.E., Howell, S.H., 1986. The virulent satellite RNA of turnip crinkle virus has a major domain homologous to the 3' end of the helper virus genome. EMBO J. 20, 3423–3428.
Simon, A.E., Roossinck, M.J., Havelda, Z., 2004. Plant virus satellite and defective interfering RNAs: new paradigms for a new century. Annu. Rev. Phytopathol. 42, 415–437.
Solorzano, A., Rodríguez-Cousiño, N., Esteban, R., Fujimura, T., 2000. Persistent yeast single-stranded RNA viruses exist in vivo as genomic RNA:RNA polymerase complexes in 1:1 stoichiometry. J. Biol. Chem. 275, 26428–26435.
Taliansky, M.E., Robinson, D.J., Murant, A.F., 2000. Groundnut rosette disease virus complex: biology and molecular biology. Adv. Virus Res. 55, 357–400.
Tamura, K., Stecher, G., Peterson, D., Filipski, A., Kumar, S., 2013. MEGA6: molecular evolutionary genetics analysis version 6.0. Mol. Biol. Evol. 30, 2725–2729.
Turina, M., Hillman, B.I., Izadpanah, K., Rastgou, M., Rosa, C., ICTV report consortium, 2017. ICTV virus taxonomy profile: Ourmiavirus. J. Gen. Virol. 98, 129–130.
Urayama, S., Kato, S., Suzuki, Y., Aoki, N., Le, M.T., Arie, T., Teraoka, T., Fukuhara, T., Moriyama, H., 2010. Mycoviruses related to chrysovirus affect vegetative growth in the rice blast fungus *Magnaporthe oryzae*. J. Gen. Virol. 91, 3085–3094.
Urayama, S., Ohta, T., Onozuka, N., Sakoda, H., Fukuhara, T., Arie, T., Teraoka, T., Moriyama, H., 2012. Characterization of Magnaporthe oryzae chrysovirus 1 structural proteins and their expression in *Saccharomyces cerevisiae*. J. Virol. 86, 8287–8295.
Urayama, S., Sakoda, H., Takai, R., Katoh, Y., Minh Le, T., Fukuhara, T., Arie, T., Teraoka, T., Moriyama, H., 2014. A dsRNA mycovirus, Magnaporthe oryzae chrysovirus 1-B, suppresses vegetative growth and development of the rice blast fungus. Virology 448, 265–273.
Vu, V.B., Takino, M., Murata, T., Nakayashiki, H., 2011. Novel vectors for retrotransposon-induced gene silencing in *Magnaporthe oryzae*. J. Gen. Plant Pathol. 77, 147–151.
Wang, M.B., Bian, X.Y., Wu, L.M., Liu, L.X., Smith, N.A., Isenegger, D., Wu, R.M., Masuta, C., Vance, V.B., Watson, J.M., Rezaian, A., Dennis, E.S., Waterhouse, P.M., 2004. On the role of RNA silencing in the pathogenicity and evolution of viroids and viral satellites. Proc. Natl. Acad. Sci. U.S.A. 101, 3275–3280.
White, K.A., Morris, T.J., 1994. Nonhomologous RNA recombination in tombusviruses: generation and evolution of defective interfering RNAs by stepwise deletions. J. Virol. 68, 14–24.
Wu, M., Zhang, L., Li, G., Jiang, D., Ghabrial, S.A., 2010. Genome characterization of a debilitation-associated mitovirus infecting the phytopathogenic fungus *Botrytis cinerea*. Virology 406, 117–126.
Zhang, X., Nuss, D.L., 2008. A host dicer is required for defective viral RNA production and recombinant virus vector RNA instability for a positive sense RNA virus. Proc. Natl. Acad. Sci. U.S.A. 105, 16749–16754.
Zuker, M., 2003. Mfold web server for nucleic acid folding and hybridization prediction. Nucleic Acids Res. 31, 3406–3415.